

Large scale inhomogeneity of inertial particles in turbulent flows

Original

Large scale inhomogeneity of inertial particles in turbulent flows / Boffetta, G.; DE LILLO, F.; Gamba, ANDREA ANTONIO. - In: PHYSICS OF FLUIDS. - ISSN 1070-6631. - STAMPA. - 16:4(2004), pp. L20-L23. [10.1063/1.1667807]

Availability:

This version is available at: 11583/1400813 since:

Publisher:

AIP

Published

DOI:10.1063/1.1667807

Terms of use:

This article is made available under terms and conditions as specified in the corresponding bibliographic description in the repository

Publisher copyright

AIP postprint/Author's Accepted Manuscript e postprint versione editoriale/Version of Record

This article may be downloaded for personal use only. Any other use requires prior permission of the author and AIP Publishing. This article appeared in PHYSICS OF FLUIDS, 2004, 16, 4, L20-L23 and may be found at <http://dx.doi.org/10.1063/1.1667807>.

(Article begins on next page)

Large scale inhomogeneity of inertial particles in turbulent flows

G. Boffetta and F. De Lillo

*Dipartimento di Fisica Generale and INFN, Università di Torino, via P. Giuria 1, 10125 Torino, Italy
and CNR-ISAC—Sezione di Torino, corso Fiume 4, 10133 Torino, Italy*

A. Gamba

Dipartimento di Matematica, Politecnico di Torino, corso Duca degli Abruzzi 24, 10129 Torino, Italy

(Received 6 October 2003; accepted 21 January 2004; published online 8 March 2004)

Preferential concentration of inertial particles in turbulent flow is studied by high resolution direct numerical simulations of two-dimensional turbulence. The formation of network-like regions of high particle density, characterized by a length scale which depends on the Stokes number of inertial particles, is observed. At smaller scales, the size of empty regions appears to be distributed according to a universal scaling law. © 2004 American Institute of Physics.

[DOI: 10.1063/1.1667807]

The transport of inertial particles in fluids displays properties typical of compressible motion even in incompressible flows. This is a consequence of the difference of density between particles and fluid. The most peculiar effect is the spontaneous generation of inhomogeneity out of an initially homogeneous distribution. The clustering of inertial particles has important physical applications, from rain generation,¹ to pollutant distribution and combustion,² to planets' formation.³ Starting from the first examples in laminar flow,⁴ it is now demonstrated both numerically^{5–7} and experimentally^{8,9} that, also in turbulent flows, there is a tendency of inertial particles to form small scale clusters. The parameter characterizing the effect of inertia is the Stokes number St , defined as the ratio between the particle viscous response time τ_s and a characteristic time of the flow τ_v . In the limit $St \rightarrow 0$ inertial particles recover the motion of fluid particles and no clusterization is expected. In the opposite limit $St \rightarrow \infty$ particles become less and less influenced by the velocity field. The most interesting situation is observed for intermediate values of St where strong clusterization is observed.^{7,8}

In the case of a smooth velocity field the Eulerian characteristic time τ_v is a well defined quantity as it can be identified with the inverse Lyapunov exponent $\tau_v = \lambda_1^{-1}$ of fluid trajectories. In this case some general theoretical predictions are possible^{10,11} such as the exponential growth of high order concentration moments. Detailed numerical simulations in a chaotic random flow have shown maximal clusterization (measured in terms of the dimension of the Lagrangian attractor) for a value $St \approx 0.1$.¹²

In the case of turbulent flow, where the velocity field is not smooth, a simple scaling argument suggests that maximal compressibility effects are produced by the smallest, dissipative scales.¹¹ Nevertheless, for sufficiently large values of St , the particle response time introduces a characteristic scale in the inertial range which breaks the scale invariance of the velocity field and produces, as we will see, large scale inhomogeneity in particle distribution.

The motion of a spherical particle in an incompressible

flow, when the radius a of the particle is so small that the surrounding flow can be approximated by a Stokes flow, is governed by the set of equations¹³

$$\begin{aligned} \dot{\mathbf{x}} &= \mathbf{v}, \\ \dot{\mathbf{v}} &= -\frac{1}{\tau_s} [\mathbf{v} - \mathbf{u}(\mathbf{x}(t), t)] + \beta \frac{d}{dt} \mathbf{u}(\mathbf{x}(t), t), \end{aligned} \quad (1)$$

where \mathbf{v} represents the Lagrangian velocity of the particle, $\beta = 3\rho_0/(\rho_0 + 2\rho)$ where ρ and ρ_0 are the density of particle and fluid, respectively, and $\tau_s = a^2/(3\nu\beta)$ is the Stokes time. The approximation of Stokes flow requires $a \ll \eta$ where η is the viscous scale of the flow. Another important assumption is that particles behave passively, i.e., their perturbation on the flow is negligible. This requires a very small mass loading, defined as the ratio of the particle mass to fluid mass.⁸ Assuming N_p particles in a cube of side L this requires $N_p a^3 \ll \beta L^3$, which can be satisfied by taking sufficiently small radius. Another constraint is obtained by requiring negligible particle interaction. This leads to a more restrictive condition on particle radius which, again, is satisfied by sufficiently small particles.¹¹

In (1) $\mathbf{u}(\mathbf{x}, t)$ represents the incompressible velocity field whose evolution is given by Navier–Stokes equations

$$\frac{\partial \mathbf{u}}{\partial t} + \mathbf{u} \cdot \nabla \mathbf{u} = -\nabla p + \nu \Delta \mathbf{u} + \mathbf{f}. \quad (2)$$

In what follows, we will consider the limit of heavy particles such that $\beta \approx 0$. In this limit it is easy to show that the Lagrangian velocity possesses a compressible part:¹¹ expanding (1) to first order in τ_s and using $\nabla \cdot \mathbf{u} = 0$, one obtains, from (2)

$$\nabla \cdot \mathbf{v} \approx -\tau_s \nabla \cdot (\mathbf{u} \cdot \nabla \mathbf{u}) \neq 0. \quad (3)$$

From (3) it is possible to give a dimensional estimation of the relative importance of the compressible part for a turbulent velocity field with scaling exponent h , $\delta_\ell u \sim U(\ell/L)^h$, L and U being a characteristic large scale and velocity. The scaling exponent for the compressible component of \mathbf{v} is

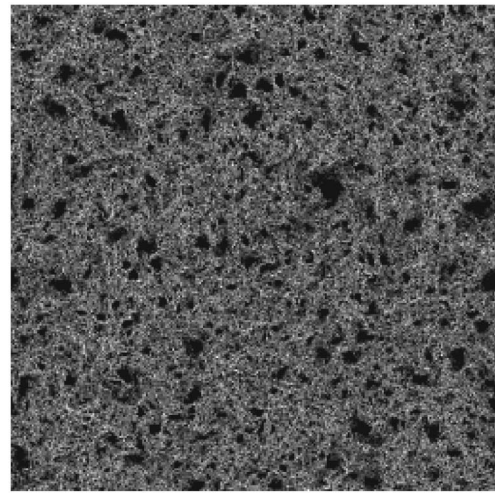
$\delta_{\ell}u \sim U(\ell/L)^{2h-1}$ and thus the relative compressibility scales as $(\ell/L)^{h-1}$, i.e., reaches the maximum value at the viscous scale η .¹¹ Nevertheless, we will see that the presence of an inertial range of scales in the turbulent flow generates large scale structures in the particle distribution at large St.

In this Letter, we address the problem of transport of heavy inertial particles in two-dimensional turbulence. There are several geophysical and astrophysical situations involving suspensions of heavy particles in two-dimensional flows, for instance the formation of planetesimals in the Solar system³ or population dynamics of plankton in the ocean.¹⁴ Most previous two-dimensional studies have been focused either on synthetic carrier flow¹⁴ or on very peculiar situations close to applications.³ Here we consider two-dimensional turbulence in the inverse energy cascade regime which displays Kolmogorov scaling on a wide range of scales. Apart from the interest for two-dimensional applications, our simulations should be also considered as a first step toward the study of turbulent transport in fully developed three-dimensional turbulence.^{15,16}

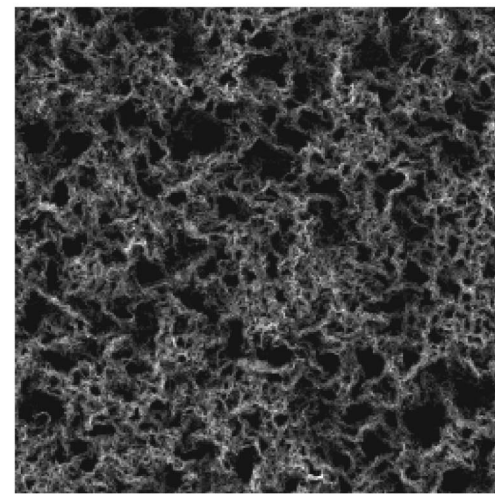
High resolution direct numerical simulations of two-dimensional Navier–Stokes equation (2) in the inverse energy cascade regime have been performed by means of standard pseudo-spectral code on a periodic box of size $L=1$ at resolution $N^2=1024^2$. Energy is injected at small scales by a random forcing \mathbf{f} with correlation function $\langle f_i(\mathbf{x},t)f_j(\mathbf{0},0) \rangle = \delta_{ij}G(t/\tau_f)F(x/\ell_f)$. The characteristic injection scale is $\ell_f \approx 0.003$ and the characteristic time τ_f is smaller than the viscous turbulent time. As customary a friction term $-\alpha\mathbf{u}$ is added to (2) in order to extract energy from the system at the friction scale $\ell_{fr} \sim \varepsilon^{1/2}\alpha^{-3/2} \approx 0.064$.¹⁷ The intermediate scales $\ell_f \ll \ell \ll \ell_{fr}$ define the inertial range in which Kolmogorov scaling $\delta_{\ell}u \sim U(\ell/L)^{1/3}$ is clearly observed.¹⁷

Lagrangian tracers are placed at random with initial zero velocity and integrated according to (1) with a given τ_s . After a scratch run long several τ_s , Lagrangian statistics is accumulated for typically some tens of τ_s . Stokes time is made dimensionless by rescaling with the Lagrangian Lyapunov exponent of fluid particles, $St \equiv \lambda_1 \tau_s$. Figure 1 shows typical distributions of inertial tracers in stationary conditions at different values of St, obtained starting from the same initial homogeneous random distribution. One observes in both cases strong inhomogeneity with empty “holes,” in the second case on much larger scales.

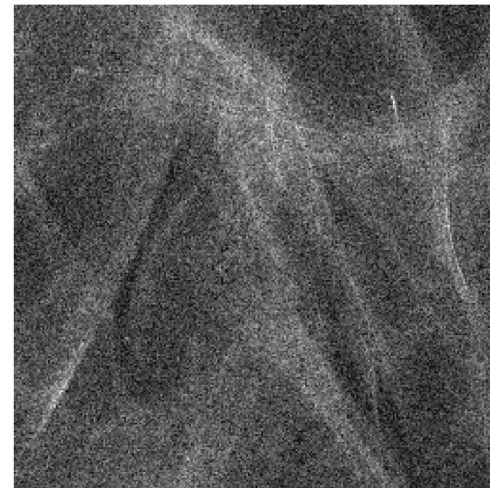
As discussed above, maximum compressibility effects are expected at small scales and can be described by the Lyapunov spectrum for inertial particles. We recall that for a generic dynamical system the sum of the Lyapunov exponents gives the exponential rate of expansion (or contraction) of the hypervolume in phase space. In our case, from (1) we have $\sum_{i=1,4}\lambda_i = -2/\tau_s$, thus volumes are contracted at a constant rate. Let us observe that when $\tau_s \rightarrow \infty$, the phase space contraction rate vanishes, and we thus expect less clusterization. As a consequence of the structure of (1) we find that two Lyapunov exponents are close to $-1/\tau_s$, representing the rate of adjustment of Lagrangian velocity to the Eulerian one. The first Lyapunov exponent is found positive, as the trajectories are chaotic and the second, negative, determines



(a)



(b)



(c)

FIG. 1. Snapshots of particle concentrations taken at the same time in stationary condition for two realizations with different Stokes numbers $St=0.12$ (a) and $St=1.2$ (b) started from identical initial conditions and advected by the same two-dimensional turbulent flow. For comparison panel (c) shows an example of particle concentration advected by a smooth flow again with $St=1.2$. The smooth turbulent flow is obtained by integrating two-dimensional Navier–Stokes equations (2) in the direct cascade regime. The number of particles in all cases is 1024^2 .

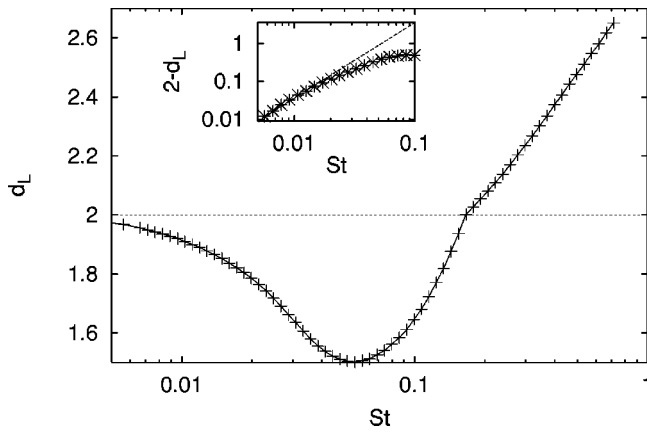


FIG. 2. Lyapunov dimension for heavy particles in two-dimensional turbulence as a function of the Stokes number. Inset: $2 - d_L$ for small St in log-log plot. Dashed line represents the St^2 behavior.

the dimension of the attractor according to the definition of Lyapunov dimension¹⁸

$$d_L = K + \frac{\sum_{i=1}^K \lambda_i}{|\lambda_{K+1}|}, \quad (4)$$

where K is defined as the largest integer such that $\sum_{i=1}^K \lambda_i \geq 0$. In Fig. 2 we show the dependence of Lyapunov dimension on Stokes number. In the limit $St \rightarrow 0$, particles become neutral and thus one recovers the homogeneous distribution with $d_L = 2$. At very small Stokes numbers, the Lyapunov dimension behaves as $d_L \approx 2 - CSt^2$ (see inset of Fig. 2) in agreement with theoretical predictions¹¹ and numerical observation in synthetic smooth flows.¹² The presence of a minimum around $St \approx 0.1$ was already discussed in the case of smooth flows¹² and indicates a value for which compressibility effects are maximum. For larger values of St particle distribution in smooth flows recovers homogeneity (see Fig. 1, right panel). We remark that the curve $d_L(St)$ of Fig. 2 is almost identical to the one obtained in smooth flows. This is a consequence of the fact that Lyapunov exponents are local quantities, describing the growth of infinitesimal separations between particles and thus insensitive to the presence of the hierarchy of scales typical of a turbulent flow.

The turbulent scenario reveals its peculiarity for larger values of St . Instead of becoming more homogeneous, the inertial particle distribution develops structures on larger scales, as is evident by comparing the central and right panels in Fig. 1. Particles are distributed on a “sponge” characterized by the presence of empty regions (holes) on different scales. This dynamical distribution of inertial particles evolves following the turbulent flow but its statistical properties are stationary. It is thus natural to study the statistics of holes at varying Stokes number.

We have performed a coarse graining of the system by dividing it into small boxes forming the sites of a square lattice and counting the number of particles contained in each small box. From this coarse grained density we have computed the probability density function of holes, defined as connected regions of empty boxes.

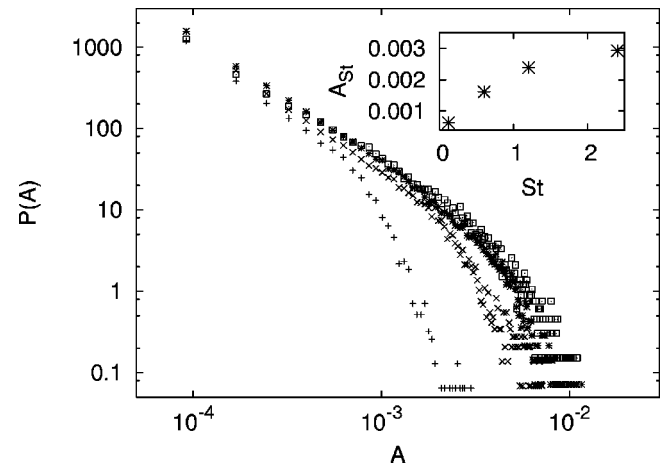


FIG. 3. Probability density functions (pdf) of hole areas, normalized with the area of the box, for $St = 0.12$ (+), $St = 0.6$ (x), $St = 1.2$ (*) and $St = 2.4$ (□). Holes are defined as connected regions of coarse grained distribution with zero density. Probability density functions are computed over 100 independent realizations of $N_p = 1024^2$ particles each. In the inset we show the dependence of the cutoff area A_{St} (defined by the condition that 1% of holes has larger area) on St . The robustness of the hole area census with respect to particle statistics have been checked by increasing the number of tracers up to 4×10^6 .

Probability density functions (pdf) of hole areas are shown in Fig. 3 for different Stokes numbers. The hole distributions follow a power law with an exponent -1.8 ± 0.2 up to an exponential cutoff at a scale A_{St} which moves to larger sizes with St , as shown in the inset of Fig. 3. At variance with the smooth flow case, in which particle density recovers homogeneity for $St > 0.1$ (Ref. 12), in the turbulent case inhomogeneities are thus pushed to larger scales when increasing St .

The hole area pdf is independent on the number of particles used in the simulations. This is a nontrivial property, reflecting the fact that inertial particles cluster on network-like structures where a clear-cut distinction between empty regions and particle-rich regions can be observed. We have also verified that the choice of the small coarse graining scale does not modify the hole area pdf at larger scales. The robustness of hole statistics with respect to particle number makes it a particularly interesting observable for experimental investigation with small mass loadings.

The presence of the cutoff A_{St} introduces a characteristic scale, $\ell_{St} \sim A_{St}^{1/2}$, in the hole distribution. When rescaled with the cutoff area, as in Fig. 4, the pdf at different St show a remarkable collapse indicating that ℓ_{St} is the only scale present in the clustering process. Increasing St , ℓ_{St} moves to larger scales (see inset of Fig. 3) until it exits the inertial range ($\ell_{St} \geq \ell_{fr}$) and self-similarity breaks down. At very large St , $\ell_{St} \gg \ell_{fr}$ and the distribution recovers the homogeneity observed in smooth flow for $St \approx 1$.

The presence of structures in the inertial particle distribution is often attributed⁵ to the fact that heavy particles are expelled from vortical regions. Although structures are related to the presence of many active scales in the turbulent flow, one should recall that in 2D turbulence, as a consequence of the direct vorticity cascade, vorticity is concen-

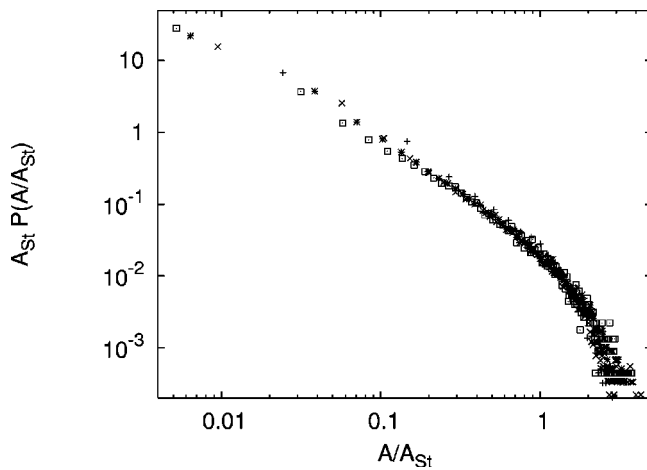


FIG. 4. Probability density functions of hole areas rescaled with the cutoff areas A_{St} computed from Fig. 3. Symbols as in Fig. 3.

trated at the small scales¹⁷ and no large scale coherent structures appear. Holes emerge as a result of the delayed dynamics (1), which filters the scales of the underlying turbulent flow characterized by times of the order of the Stokes time τ_s .

As discussed before, clustering occurs also in synthetic flows where a hierarchy of time scales is absent, just as a consequence of the dissipative character of the motion.¹² However, it appears from our simulations that to fully understand the geometry of inertial particle distribution in a turbulent flow the presence of structures characterized by a large set of time scales cannot be ignored.

We conclude that the geometry of inertial particle clusters in developed turbulence is controlled both by the dissipative effective dynamics of the particle motion at small scales, and by the tendency of inertial particles to filter the active scales characterized by times of the order of the characteristic relaxation time of the particles. A full understanding of the geometry of particle clusters in developed turbulence is particularly relevant for several applications, such as coalescence processes or chemical reactions. The reaction rate of two chemical species is a function of their concentration. When particles of different species are transported by the same turbulent flow, their local concentrations are not

independent and the presence of large scale correlations in the particle distribution can in principle influence the reaction velocity.

ACKNOWLEDGMENTS

We acknowledge the allocation of computer resources from INFN "Progetto Calcolo Parallelo." We thank an anonymous referee for many useful remarks.

- ¹G. Falkovich, A. Fouxon, and M.G. Stepanov, "Acceleration of rain initiation by cloud turbulence," *Nature* (London) **419**, 151 (2002).
- ²R.W. Dibble, J. Warnatz, and U. Maas, *Combustion: Physical and Chemical Fundamentals, Modeling and Simulations, Experiments, Pollutant Formation* (Springer, New York, 1996).
- ³A. Bracco, P.H. Chavanis, A. Provenzale, and E.A. Spiegel, "Particle aggregation in a turbulent Keplerian flow," *Phys. Fluids* **11**, 2280 (1999).
- ⁴M. Maxey, "The gravitational settling of aerosol particles in homogeneous turbulence and random flow fields," *J. Fluid Mech.* **174**, 441 (1987).
- ⁵K.D. Squires and J.K. Eaton, "Preferential concentration of particles by turbulence," *Phys. Fluids A* **3**, 1169 (1991).
- ⁶L.P. Wang and M. Maxey, "Settling velocity and concentration distribution of heavy particles in homogeneous, isotropic turbulence," *J. Fluid Mech.* **256**, 27 (1993).
- ⁷R.C. Hogan and J.N. Cuzzi, "Stokes and Reynolds number dependence of preferential particle concentration in simulated three-dimensional turbulence," *Phys. Fluids* **13**, 2938 (2001).
- ⁸J.R. Fessler, J.D. Kulick, and J.K. Eaton, "Preferential concentration of heavy particles in a turbulent channel flow," *Phys. Fluids* **6**, 3742 (1994).
- ⁹A. Aliseda, A. Cartellier, F. Hainaux, and J.C. Lasheras, "Effect of preferential concentration on the settling velocity of heavy particles in homogeneous isotropic turbulence," *J. Fluid Mech.* **468**, 77 (2002).
- ¹⁰T. Elperin, N. Kleorin, and I. Rogachevskii, "Self-excitation of fluctuations of inertial particle concentration in turbulent fluid flow," *Phys. Rev. Lett.* **77**, 5373 (1996).
- ¹¹E. Balkovsky, G. Falkovich, and A. Fouxon, "Intermittent distribution of inertial particles in turbulent flows," *Phys. Rev. Lett.* **86**, 2790 (2001).
- ¹²M.J. Bec, "Fractal clustering of inertial particles in random flow," *Phys. Fluids* **15**, L81 (2003).
- ¹³M. Maxey and J. Riley, "Equation of motion for a small rigid sphere in a nonuniform flow," *Phys. Fluids* **26**, 883 (1983).
- ¹⁴T. Nishikawa, Z. Toroczkai, C. Grebogi, and T. Tel, "Finite-size effects on active chaotic advection," *Phys. Rev. E* **65**, 026216 (2002).
- ¹⁵G. Boffetta and I.M. Sokolov, "Statistics of two-particle dispersion in two-dimensional turbulence," *Phys. Fluids* **14**, 3224 (2002).
- ¹⁶A. Celani, A. Lanotte, A. Mazzino, and M. Vergassola, "Fronts in passive scalar turbulence," *Phys. Fluids* **13**, 1768 (2001).
- ¹⁷G. Boffetta, A. Celani, and M. Vergassola, "Inverse energy cascade in two-dimensional turbulence: Deviations from Gaussian behavior," *Phys. Rev. E* **61**, R29 (2000).
- ¹⁸E. Ott, *Chaos in Dynamical Systems* (Cambridge University Press, New York, 1993).